



1/f Noise in the superconducting transition of a MgB₂ thin film

B. Lakew^a, S. Aslam^{a,*}, H. Jones^b, T. Stevenson^c, N. Cao^{c,d}

^a NASA/Goddard Space Flight Center, Planetary Systems Laboratory, Code 693, Greenbelt, MD 20771, USA

^b NASA/Goddard Space Flight Center, Microwave Instrument & Technology Branch, Code 555, Greenbelt, MD 20771, USA

^c NASA/Goddard Space Flight Center, Detector Systems Branch, Code 553, Greenbelt, MD 20771, USA

^d MEI Technologies Inc., 2525 Bay Area Blvd., Houston, TX 77058, USA

ARTICLE INFO

Article history:

Received 9 December 2009

Accepted 20 March 2010

Available online 27 March 2010

Keywords:

MgB₂ thin film

Bolometer

Noise spectral density

1/f Noise

Excess noise

ABSTRACT

The noise voltage spectral density in the superconducting transition of a MgB₂ thin film on a SiN-coated Si thick substrate was measured over the frequency range 1 Hz to 1 kHz. Using established bolometer noise theory the theoretical noise components due to Johnson, 1/f (excess) and phonon noise are modeled to the measured data. It is shown that for the case of a MgB₂ thin film in the vicinity of the mid-point of transition, coupled to a heat sink via a fairly high thermal conductance ($\approx 10^{-1}$ W/K) that the measured noise voltage spectrum is 1/f limited and exhibits 1/f^a dependence with *a* varying between 0.3 and 0.5 in the measured frequency range. At a video frame rate frequency of 30 Hz the measured noise voltage density in the film is ≈ 61 nV/ $\sqrt{\text{Hz}}$, using this value an upper limit of electrical NEP ≈ 0.67 pW/ $\sqrt{\text{Hz}}$ is implied for a practical MgB₂ bolometer operating at 36.1 K.

Published by Elsevier B.V.

1. Introduction

The signal-to-noise performance of a bolometer that uses the resistive transition of a superconducting film as a temperature sensor (thermistor) is limited by incoherent noise sources. Ideally a fully optimized bolometer should be designed such that the dominant noise sources are Johnson and phonon noise [1]. However, superconducting films that are used in bolometer construction are generally polycrystalline and granular in nature and can give rise to large current dependant excess noise, it is therefore important to assess the 1/f noise contribution from the film itself. Many reports in the literature have shown that in high-*T_c* superconducting granular ceramic thin films, e.g. YBCO, that the excess noise approaches zero in the superconducting state and that it rises sharply in the transition region with a 1/f^a type spectrum with *a* ≤ 1 over a wide range of frequencies [2]. Gandini et al. [3] have reported similar findings for a granular MgB₂ thin film sample, they postulate a percolation process between grains in the film for the origin of the noise and show 1/f^a noise dependence with *a* ≈ 1.5 in the range 1–100 Hz. In addition to the film intrinsic noise, the thermal coupling between the film and the substrate also plays an important role in determining both the noise magnitude and the shape of the spectrum [4]. In this paper we present results of a noise voltage spectral density measurement in the superconducting transition of a high resistance MgB₂ thin film on a bulk SiN-

coated Si thick substrate in order to establish whether or not the level of excess noise from the film alone will limit the ultimate detection sensitivity when used in a bolometer construction.

2. High-*T_c* superconducting bolometer noise

In a high-*T_c* bolometer incoming radiation, P_{rad} [W], heats up an absorber and changes the electrical resistance, R [Ω], of a thermistor with a temperature coefficient of resistance (TCR), $\alpha = (1/R)(dR/dT)$ [K^{-1}]. The absorber with heat capacity C [J/K] is weakly coupled through a link with a thermal conductance G [W/K] to a cold thermal reservoir at temperature T_0 . The resulting thermal time constant is $\tau = C/G$ [s]. The electrical resistance change modifies the Joule heating, $P_{bias} = I_{bias}V$ [W], giving rise to an Electro-Thermal Feedback (ETF) [5–7] into the bolometer that produces an effective thermal conductance $G_e = G(1 - L_0)$ [W/K] and an effective time constant of $\tau_e = \tau/(1 - L_0)$ [s] where $L_0 = \alpha P_{bias}/G$ is a dimensionless parameter that can be considered as the loop gain in the ETF mechanism. Assuming that phonon noise from background radiation, measurement system noise sources and noise due to acoustic bubbling in the liquid He cooling bath are small enough to be ignored [1], then the three main fundamental uncorrelated noise sources in the bolometer are Johnson and 1/f (current or excess) noise of the thermistor resistance and phonon noise of the link to the cold thermal reservoir. Mather [5] has noted the effect of the ETF on the noise properties of the bolometer, using his treatment the noise voltage spectral density due to Johnson noise, $S_f(\omega)$, can be derived as,

* Corresponding author. Tel.: +1 301 286 1330.

E-mail address: shahid.aslam-1@nasa.gov (S. Aslam).

$$S_j(\omega) = \left[4k_B T R \cdot \frac{1 - L_0^2 + \omega^2 \tau^2}{(1 - L_0)^2 + \omega^2 \tau^2} \right]^{1/2} \quad (1)$$

The thermistor thin film resistance and its quality (e.g. grain size, non-uniformities, etc.) also gives rise to $1/f^a$ noise [4]. The exponent, a , generally for e.g. high- T_c YBCO thin films is in the range between 0.6 and 0.9 [8]. Assuming that the $1/f$ noise power spectral density, $S_{1/f}^2(\omega)$ [V 2 /Hz], follows a frequency dependence of f^{-1} and that $S_{1/f} \propto I_{bias}$ [9], then the corresponding $1/f$ noise voltage spectral density, $S_{1/f}(\omega)$ [V/Hz] after some computation can be expressed as,

$$S_{1/f}(\omega) = \frac{\sqrt{4k_B T G L_0 \alpha^{-1} \omega_0 \omega^{-1}}}{I_{bias}} \quad (2)$$

Fluctuations in the thermal equilibrium mean square energy in the thermistor thin film give rise to a phonon noise voltage spectral density, $S_p(\omega)$ [V/Hz], given by [7],

$$S_p(\omega) = \sqrt{4k_B T^2 G} \cdot \mathfrak{R}_v(\omega) \quad (3)$$

In the above equations, k_B is the Boltzmann constant and $\omega = 2\pi f$ [Hz] is the angular frequency. The second term in Eq. (3) is the voltage responsivity, $\mathfrak{R}_v(\omega) = \eta L_0 / (I_{bias}(1 - L_0) \sqrt{1 + \omega^2 \tau_c^2})$ [V/W] where $\eta = 1$ for 100% radiation absorption efficiency and in Eq. (2) $\omega_0 = 2\pi f_0$ [Hz] is the angular corner frequency, i.e. the transition from $1/f$ to phonon noise for a fixed I_{bias} , determined from the log-log plot of the measured noise voltage spectral density. It is noted that $1/f$ noise of Eq. (2) and phonon noise of Eq. (3) is not measurable without a bolometer bias current, whereas Johnson noise from Eq. (1) is always present. Since, the contributions of Johnson, $1/f$ and phonon noise are uncorrelated, the mean-square values will add to give the total equivalent noise voltage spectral density, $S_t(\omega)$ [V/Hz],

$$S_t(\omega) = \left[\langle S_j(\omega) \rangle^2 + \langle S_{1/f}(\omega) \rangle^2 + \langle S_p(\omega) \rangle^2 \right]^{1/2} \quad (4)$$

Eq. (4) is used to define the Noise Equivalent Power, NEP [W/Hz], of a bolometer, i.e. $NEP_t = S_t(\omega) / |\mathfrak{R}_v(\omega)|$ [1]. A plot of NEP_t as a function of thermal conductance, G , is shown in Fig. 1a for a low noise MgB_2 thin film based bolometer that has a corner frequency of $f_0 = \omega_0/2\pi = 2$ Hz and the following realizable parameters, $C = 1$ nJ K $^{-1}$, $L_0 = 0.3$, $\alpha = 1.67$ K $^{-1}$, $R = 1$ K Ω , $T = 36.1$ K and $I_{bias} = \sqrt{L_0 G / \alpha R}$, operating at a video frame rate frequency $f = 30$ Hz. Also shown in this figure are the NEP contributions from Johnson, $1/f$ and phonon noise to highlight the fact that for this case NEP_t is phonon and Johnson noise limited. However, for the case of a noisier film, i.e. if the corner frequency is increased to $f_0 = 2$ kHz then with all other parameters remaining the same, NEP_t increases and becomes $1/f$ noise limited, see Fig. 1b. This figure also shows that the upper limit of $1/f$ noise in a thin film on a substrate with large G can be established with some confidence.

3. Experiment

3.1. Sample preparation

MgB_2 thin film of thickness 200 nm was deposited by the reactive evaporation growth technique [10] onto a 4-in. SiN-coated silicon wafer. The MgB_2 thin film was then patterned into high resistance elements using standard photolithography and a nitric acid etch technique [11]. A photograph of the patterned line structure with dimensions is shown Fig. 2. The typical resistance of a patterned element was nominally 4.25 K Ω . Four resistance elements were stitched together in series using gold wire bonding to make a total resistance of 17.35 K Ω (at room temperature). The larger resistance is needed in order to ensure that the noise

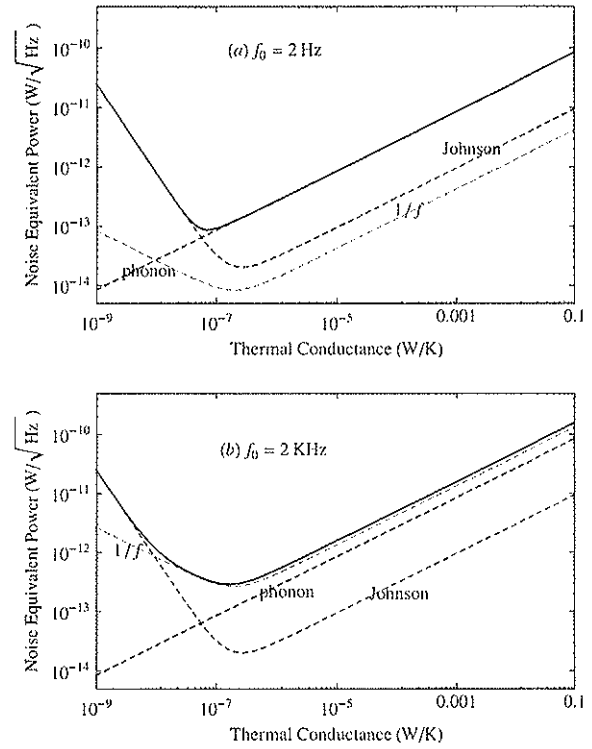


Fig. 1. Theoretical NEP as a function of thermal conductance for: (a) low noise film with a corner frequency of $f_0 = 2$ Hz showing phonon and Johnson noise limit and (b) higher noise film with $f_0 = 2$ KHz showing $1/f$ noise limit.

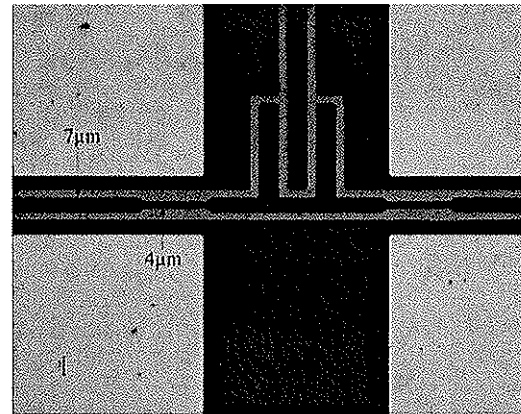


Fig. 2. Photograph of a portion of a patterned MgB_2 resistance element. The total length (not shown) of the line is 14.159 mm; the measured resistance is nominally 4.25 K Ω at room temperature.

generated from the resistive sample is above the noise floor of the LNA used in the measurement system, this avoids using a blocking capacitor and matching transformer. The sample was mounted onto a thermal standoff in a blanked off He cryogen cooled dewar. Resistance as a function of temperature was measured using the standard four-wire technique.

3.2. Noise measurement system

A block diagram of the noise measurement system is shown in Fig. 3a, it consists of a SRS 560 Low Noise Amplifier (LNA) at a gain of 10,000 and a HP3567A spectrum analyzer to read and calculate

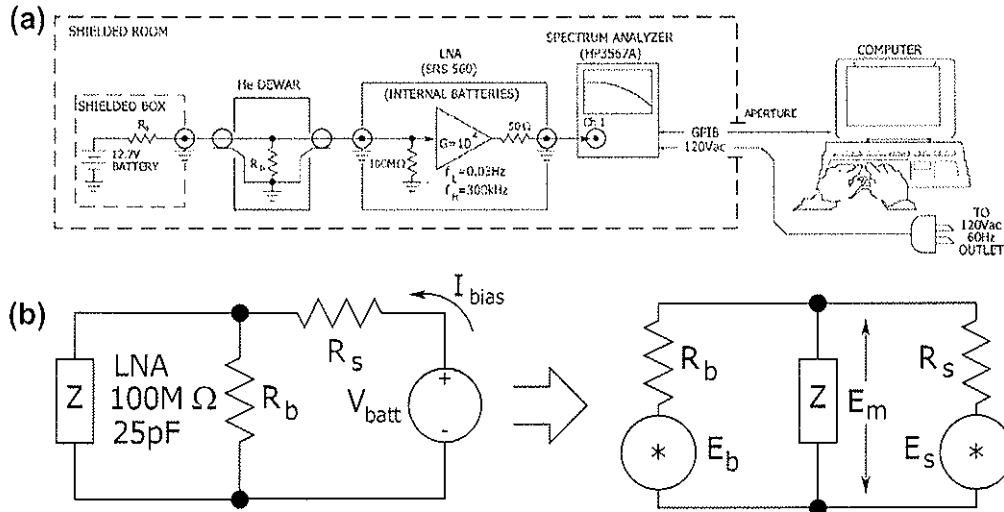


Fig. 3. (a) Block diagram of the noise measurement system and (b) schematic of current bias circuit set-up and its equivalent circuit.

the power spectral density of the MgB_2 thin film resistor. A battery in series with a low-noise wire wound resistor in a shielded box provides a near-constant current to the MgB_2 bolometer for most measurements, i.e. when $R_s \gg R_b$. The noise measurement system is housed in a Faraday room to cut down extraneous 60 Hz pickup. The sample is mounted onto a thermal standoff in a blanked off He-cryogen dewar, which also provides extra shielding. The LNA runs on internal batteries, however the shielded 120 V 60 Hz power and a GPIB communication cables are routed inside through an aperture in the shielded room to the spectrum analyzer. A computer outside the shielded room controls and captures data from the spectrum analyzer. The measurement system was assessed for accuracy prior to noise voltage data collection on the sample, this included: (i) performing swept sine frequency responses at various input resistances (from 10 m Ω to 10 K Ω) to obtain amplitude gain versus frequency curves; (ii) establishing the LNA noise performance, by taking 3000 averages on the spectrum analyzer when the LNA input is shorted to obtain the equivalent noise voltage and also when the LNA is terminated with a 1 G Ω impedance to obtain the equivalent current noise and finally (iii) calibrating the measurement system by using Johnson noise sources, i.e. 1 k Ω and 10 k Ω terminations at room temperature thus establishing no more than a 4% deviation from calculated Johnson noise values.

3.3. Noise spectral density data correction due to bias circuit

When the source resistance R_s (bias resistor at room temperature) is the same order as the bolometer resistance R_b then the measured noise voltage across the bolometer collected by the spectrum analyzer has to be corrected to account for this. Fig. 3b shows a schematic of the bias circuit set-up and shows the battery-driven current through R_s and R_b with the high impedance LNA in parallel. Shorting the battery and inserting noise generators, E_b and E_s , in series with R_b and R_s , respectively helps to determine the noise contribution from the source resistance. With the amplifier, Z element, in the center, a familiar mesh circuit is revealed that can be solved easily by the superposition method. The equivalent voltage noise, E_m , generated by element Z is known through measurement. Applying the superposition method and after some computation and converting the measured noise voltage, E_m , bolometer noise voltage, E_b , and source noise voltage, E_s , into spectral densities, $S_m(\omega)$, $S_b(\omega)$, $S_s(\omega)$ respectively and assuming that $|Z| \rightarrow \infty$ and

that $S_s(\omega)$ is strictly Johnson noise (i.e. no $1/f$ noise component from the source resistance), gives $S_b(\omega)$ the noise voltage spectral density of the bolometer itself,

$$S_b(\omega) = \left[\left(S_m(\omega) \cdot \frac{R_s + R_b}{R_s} \right)^2 - \left(S_s(\omega) \cdot \frac{R_b}{R_s} \right)^2 \right]^{1/2} \quad (5)$$

In Eq. (5), R_b , R_s , $S_s(\omega)$ and $S_m(\omega)$ are known through measurement and post processing, $S_b(\omega)$ then represents the corrected noise voltage spectral density. For the condition $R_s \gg R_b$ Eq. (5) simplifies to $S_b(\omega) \approx S_m(\omega)$; and when $R_s = R_b$ then $S_m(\omega) = \sqrt{4S_m^2(\omega) - S_s^2(\omega)}$.

4. Measurement results

4.1. MgB_2 thin film transition curve

The MgB_2 thin film resistance as a function of temperature in the superconducting transition region together with its first derivative, dR/dT , is shown in Fig. 4. The resistance was measured using a bias current of $I_{\text{bias}} = 10 \mu\text{A}$. The transition curve shows an extra inflexion point near the mid of transition, the dR/dT curve consequently shows an uncharacteristic minima at 36.35 K, this is due to the sample being constructed from four resistive element's connected in series to form a high resistance sample. This anomalous feature is most likely due to each of the four elements having slightly different critical transition temperatures. The room temperature sample resistance was $R_{295\text{K}} = 17.35 \text{ K}\Omega$ and at near superconducting transition, 40 K, was $R_{40\text{K}} = 9.87 \text{ K}\Omega$ giving a resulting residual resistance ratio of $R_{295\text{K}}/R_{40\text{K}} = 1.8$. Near the mid-point of transition, at a temperature $T_m = 36.1 \text{ K}$ the sample resistance is $R_m = 4.5 \text{ K}\Omega$, $dR/dT = 7.54 \text{ K}\Omega/\text{K}$ and the TCR is $\alpha = 1.67 \text{ K}^{-1}$.

4.2. Calculation of MgB_2 thin film heat capacity and thermal conductance of substrate

The sample consists essentially of a MgB_2 thin film of thickness 200 nm lying on a SiN-coated Si substrate of thickness 380 μm attached, using GE varnish, to a circuit board made out of G10 material of thickness 1 mm; the G10 board is attached to the heat sink using self-adhesive copper tape. For the case of a thin metallic film

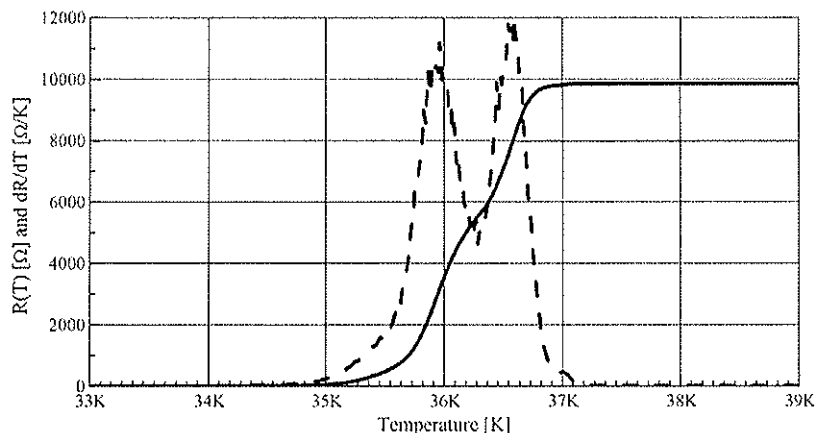


Fig. 4. Electrical resistance transition and dR/dT for a sample composed of four MgB_2 resistance elements serially connected.

(>100 nm) on a dielectric coated thick substrate at a temperature ≈ 40 K the phonon modes in the combined system are strongly coupled and the Kapitza boundary resistance between the film and substrate can be considered small [12] hence the heating and cooling of the film is largely dependent on the thermal conductivity properties of the substrate. In the experimental set-up the contribution from radiation transfer is assumed negligible since the sample is housed in a cold enclosure. Carr et al. [13] have observed that the time constant, τ , for YBCO thin films is proportional to the film thickness, this indicates that the thermal capacity contribution from the thin film itself is sufficient for a first-order calculation. For bulk sintered MgB_2 the specific heat capacity is $c \approx 20$ J/kg/K at 40 K [14] and the density is $\rho = 2550$ Kg/m³ [15]; these values were used since no reliable cryogenic thermo-physical data for MgB_2 thin films in the literature is known. For the four resistive elements in series that constitutes the sample the total volume of the MgB_2 thin film is $V = 1.98 \times 10^{-14}$ m³ giving a total thermal capacity $C = c\rho V \approx 4 \times 10^{-9}$ J/K. Comparing the thermal conductance values at 40 K for Si, SiN and G10, i.e. $k_{Si} = 3530$ W m⁻¹ K⁻¹, $k_{SiN} = 1.58$ W m⁻¹ K⁻¹, $k_{G10} = 0.21$ W m⁻¹ K⁻¹, respectively, it is clear that the thermal impedance, (G^{-1}), to the heat sink is dominated by the G10 board. Using the G10 thermal conductivity value yields a thermal conductance of $G_{G10} = 7.66 \times 10^{-2}$ W K⁻¹. The gold wire bonds that make electrical connections and self-adhesive copper tape for fixing the G10 board to the heat sink also add to the thermal conductance, the estimated contribution is $G_{misc} \approx 3.8 \times 10^{-2}$ W K⁻¹, giving a total thermal conductance of $G \approx 1.1 \times 10^{-1}$ W K⁻¹. This gives a very fast response with a thermal time constant of $\tau \approx 3.5 \times 10^{-8}$ s. However, the total thermal conductance, G , is very large resulting in a relatively low voltage responsivity ($\mathfrak{R} \propto \alpha \cdot G^{-1}$) and a high noise equivalent power ($NEP \propto \sqrt{G}$) resulting in a poor performance bolometer. These results are not surprising since the sample under study was not fabricated as a high sensitivity bolometer with optimal performance but rather to quantify the upper limit of excess noise in the MgB_2 thin film.

4.3. Noise voltage spectral density of MgB_2 thin film at mid-point of transition

The noise voltage spectral density was measured just below the mid-point inflexion point at temperature $T_m = 36.1$ K where $dR/dT = 7540$ Ω K⁻¹ and $\alpha = 1.67$ K⁻¹. The spectrum analyzer averaged 250 spectral density measurements in the frequency range 0.1 Hz to 1.6 KHz. The collected raw data was smoothed using interpolation and median filters to within <5% error and subjected to gain

correction and subtraction in quadrature of the measurement system equivalent noise and bias circuit noise contribution. Fig. 5a shows the smoothed and corrected noise voltage density, $S_b(\omega)$, spectra between 1 Hz and 1 KHz. The noise voltage exhibits f^a dependence, with $a \approx 0.5$ between 1 Hz and 40 Hz and $a \approx 0.3$ between 40 Hz and 1 KHz. In Fig. 5b the theoretical noise voltage spectra due to contributions from phonon noise of the thermal conductance, $S_\nu(\omega)$, Johnson noise due to the bolometer resistance (cf $\sqrt{4kT_0R_m} \approx 3$ nV/ $\sqrt{\text{Hz}}$), $1/f$ noise of the film, $S_{1/f}(\omega)$, and the theoretical total noise voltage density, $S_t(\omega)$, are plotted using Eqs. (1)–(4) and superimposed on the corrected voltage spectral

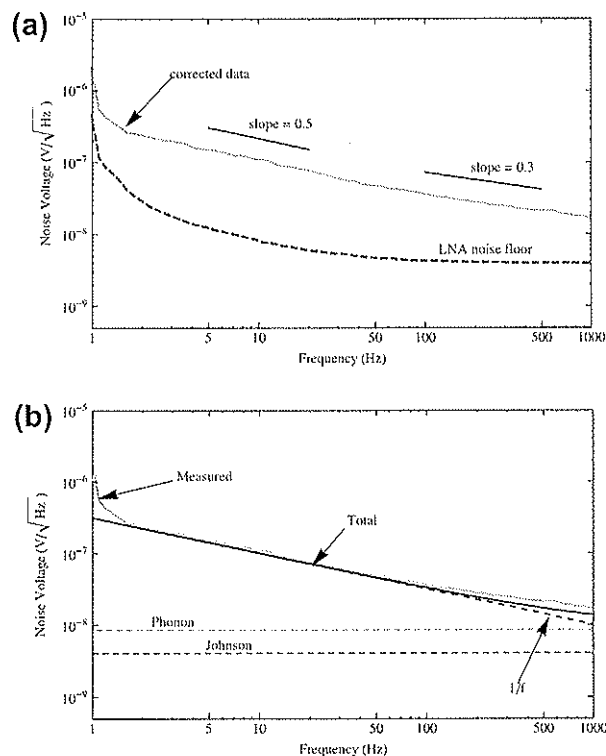


Fig. 5. (a) Corrected noise voltage spectral density of MgB_2 film sample at 36.1 K in the superconducting transition and LNA noise floor and (b) theoretical Johnson, phonon and $1/f$ noise contributions and fit to the measured data. The model parameters are, $L_0 = 0.3$, $\alpha = 1.67$ K⁻¹, $G = 1.15 \times 10^{-1}$ W K⁻¹, $I_b = 0.5$ mA, $T_0 = 36.1$ K, $\tau = 35$ ns and $f_0 = 2$ KHz.

Table 1

Measured and theoretical noise contributions at 10 Hz, 30 Hz and 50 Hz for a MgB₂ film at $T_0 = 36.1$ K, $R_m = 4.5$ K Ω and $C = 1.15 \times 10^{-1}$ WK⁻¹.

Noise component (nV/ $\sqrt{\text{Hz}}$)	Frequency		
	10 Hz	30 Hz	50 Hz
Measured	108.98	60.12	47.05
Johnson	4.08	4.08	4.08
1/f	99.63	57.52	44.55
Phonon	17.05	17.06	17.06
Ratio of Johnson-to-1/f	1:24	1:14	1:11
Ratio of Johnson-to-measured	1:27	1:15	1:12

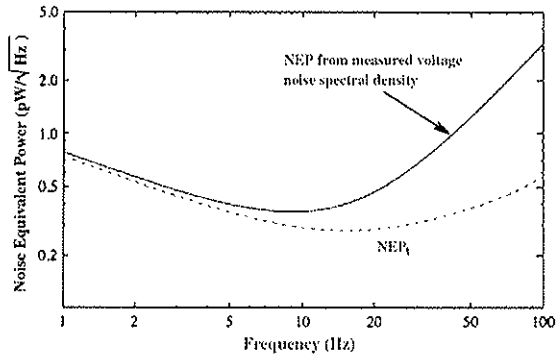


Fig. 6. Upper bound of NEP derived from measured noise voltage spectral density.

density. This figure shows that the frequency dependence of the measured noise voltage is very well described by Eq. (4) and that the measured noise is close to the theoretical limit of $1/f$ noise of the film. A power law curve fit gives the noise voltage level between 2 Hz and 100 Hz, i.e. $S_b(f) = (3.325 \times 10^{-7}) \cdot f^{-0.492}$ and thus from Fig. 5b the level of excess noise above the theoretical Johnson noise can be deduced. Table 1 gives the ratios of Johnson-to- $1/f$ and Johnson-to-measured noise at modulation frequencies 10 Hz, 30 Hz, and 50 Hz and for comparison the values of theoretical Johnson, phonon and $1/f$ noise are also tabulated. Since the noise voltage spectrum was measured on a substrate with high thermal conductance to the heat sink, the noise level measured represents an upper bound for any practical bolometer that has a thermal conductance orders of magnitude lower, see Fig. 1b. The measured noise voltage spectrum, see Fig. 5b, can therefore be used to establish an upper bound of NEP . Fig. 6 shows a plot of the NEP as a function of frequency using the measured noise voltage spectrum and the following bolometer parameters, $C = 1$ nJ/K, $R = 4.5$ K Ω , $L_0 = 0.3$, $\alpha = 1.67$ K⁻¹, $T = 36.1$ K, $f_0 = 2$ KHz and $I_{bias} = (L_0 C / \alpha R)^{1/2}$ operating at a modulation frequency, $f = 30$ Hz. On the same plot the total theoretical NEP_t using the same parameters as above is shown calculated from Eq. (4) for comparison. It is seen that the measured excess noise of the film at 30 Hz increases the NEP by just over a factor of two from the theoretical value, i.e. from

0.31 pW/ $\sqrt{\text{Hz}}$ to 0.67 pW/ $\sqrt{\text{Hz}}$ for a film with a corner frequency $f_0 = 2$ KHz.

5. Summary

The noise voltage spectral density in a MgB₂ thin film with resistance $R_m = 4.5$ K Ω , near the mid-point of superconducting transition, at $T_m = 36.1$ K was measured between 1 Hz and 1 kHz with a constant current bias of $I_{bias} = 0.5$ mA. The noise voltage spectrum showed $\approx 1/f^{0.5}$ dependence between 2 and 100 Hz, a corner frequency of $f_0 \approx 2$ kHz and a noise voltage spectral density of $S_b = 60.12$ nV/ $\sqrt{\text{Hz}}$ at a video frame rate frequency of 30 Hz. The upper bound for the electrical NEP of a practical bolometer constructed from a MgB₂ thin film with this noise level was calculated to be $NEP = 0.67$ pW/ $\sqrt{\text{Hz}}$. Assuming a radiation absorbing area of $A = 1$ mm² with an absorption efficiency of $\eta = 0.5$ (space matched coating) in the spectral wavelength range 20–100 μm , then gives a specific detectivity, $D' = (\eta \sqrt{A} / NEP) \approx 7.5 \times 10^{10}$ cm $\sqrt{\text{Hz}}/\text{W}$. For comparison, Portesi et al. [16] have reported on a MgB₂ bolometer operating at 32.4 K with no separate absorber with a $D' = 2 \times 10^{10}$ cm $\sqrt{\text{Hz}}/\text{W}$, when measured with a chopped 785 nm radiation source at 8 Hz. It is predicted that as MgB₂ polycrystalline thin film growth techniques improve to give smooth films with nanometer grain sizes that exhibit a $1/f$ noise corner frequency of 2 Hz or less, then the relative contribution of $1/f$ noise will be greatly reduced and an optimized phonon noise limited bolometer with a $D' = 1.6 \times 10^{11}$ cm $\sqrt{\text{Hz}}/\text{W}$ or better will be realized.

Acknowledgements

The authors wish to thank W.-T. Hsieh (NASA, GSFC) for fabrication processing advice and B. H. Moeckly (Superconducting Technologies Inc.) for the deposition of MgB₂ thin films.

References

- [1] P.L. Richards, J. Appl. Phys. 76 (1994) 1.
- [2] J.H. Lee, S.C. Lee, Z.G. Khim, Phys. Rev. B 40 (1989) 6806.
- [3] C. Gandini, M. Rajteri, C. Portesi, E. Monticone, A. Masoero, P. Mazzetti, in: J. Phys.: 7th European Conference on Applied Superconductivity, Conference Series, vol. 43, 2006, pp. 313–316.
- [4] P. Dutta, P.M. Horn, Rev. Mod. Phys. 53 (3) (1981) 497.
- [5] J.C. Mather, Appl. Opt. 21 (1982) 1125.
- [6] K. Irwin, Appl. Phys. Lett. 66 (1995) 1998.
- [7] M.J.M.E. de Nivelie et al., J. Appl. Phys. 82 (10) (1997) 4719.
- [8] T. Nguyen, J.M. O'Callaghan, B.A. Davidson, R.D. Redwing, G.K.G. Hohenwarter, J.E. Nordman, J.B. Beyer, IEEE Trans. Appl. Supercond. 5 (2) (1995) 3369.
- [9] P. Dutta, J.W. Eberhard, P.M. Horn, Solid State Commun. 27 (1978) 1389.
- [10] B.H. Moeckly, W.S. Ruby, Supercond. Sci. Technol. 19 (2006) L21.
- [11] S. Aslam, T.R. Stevenson, W. T Hsieh, D. E Travers, H. H Jones, B. Lakew, IEEE Trans. Appl. Supercond. 19 (1) (2009).
- [12] J.T. Karvonen, I.J. Maasilta, J. Phys., Con. Ser. 92 (2007) 01 2043.
- [13] G.L. Carr, M. Quijada, D.B. Tanner, C.J. Hirschmugl, G.P. Williams, S. Etemad, B. Dutta, R. DeRossa, A. Inam, T. Venkatesan, X. Xi, Appl. Phys. Lett. 57 (1990) 2725.
- [14] R.K. Kremer, B.J. Gibson, K. Ahn, <http://arxiv.org/abs/cond-mat/0102432v2>.
- [15] S.L. Bud'ko, G. Lapertot, C. Petrovic, C.E. Cunningham, N. Anderson, P.C. Canfield, Phys. Rev. Lett. 86 (2001) 1877.
- [16] C. Portesi, E. Taralli, R. Introzzi, M. Rajteri, E. Monticone, Supercond. Sci. Technol. 20 (2007) S403.